Wen Ren*
Xia Wen
Sencai Lai

Digital Real-Time Rotating Speed Measuring and Fuzzy PID Control Algorithm Design for the Multi-Speed Electronic Let-Off System

DOI: 10.5604/01.3001.0014.8231

Sanming University,
College of Mechanical and Electrical Engineering,
Sanming, Fujian 365004, China
* e-mail: auwren@foxmail.com

Abstract
Aiming at the warp knit fabric horizontal strip problem faced by the multi-speed electronic let-off process of warp knitting machines, a design scheme of a fully digital intelligent multi-speed electronic system is proposed. A wide-range digital speed measurement method is proposed which solves the problem that the traditional analog circuit speed measurement method cannot measure the real-time warp beam speed, and also eliminates the problem of the low-speed feedback blind zone. According to the characteristics of the electronic let-off system of warp knitting machines, the hardware structure and software algorithm of the fuzzy PI control system were designed which can adjust the control parameters of the traditional PI controller in real time according to the fuzzy control table, and realise stable multi-speed electronic let-off. The effectiveness of the design method was verified by simulation.

Key words: *warp knitting machine; digital real-time speed measuring; multi-speed electronic let-off control system; fuzzy PI control algorithm.*

Introduction

The warp let-off system is one which unwinds the warp from the warp beam and feeds it into the loop-forming mechanism according to a certain let-off amount [1]. It is one of the most important components of a warp knitting machine, which directly affects the quality and pattern varieties of warp knitting products, and is also the key technology of electronic traverse and electronic jacquard systems [2]. The feature and advantage of the multi-speed electronic let-off system lies in its ability to produce complex pattern fabrics, which is the leading development direction of the current electronic let-off system for warp knitting machines [3, 4]. In the production process of multi-speed warp knitting, a variety of let-off amounts (sequences) need to be knitted. The warp beam motor must respond quickly during each sequence switching to achieve a sudden change in the let-off amount. If the response speed of the motor is not fast enough or it is not stable enough this will cause the warp yarn tension to fluctuate, and there will be obvious horizontal stripes on the cloth surface, which affects the product quality. Therefore, it is necessary to establish a control strategy suitable for the multi-speed electronic let-off system.

Tachometer generators, photoelectric encoders and Hall elements are widely used warp beam drive motor speed measurement devices. Speed measurement accuracy plays a vital role in the performance of the warp knitting machine multi-speed let-off control system [5, 6]. As a commonly used analog speed measuring device, the cost-effective tachogenerator can convert the mechanical speed of the motor into an electrical signal, which is widely used in various speed or position control systems [7]. The traditional analog speed measurement method using a tachometer generator is as follows: the sinusoidal voltage wave output by the tachometer generator is converted into an average analog level signal reflecting the speed of the measured motor through a single-phase bridge-type controllable rectifier circuit and filter circuit, which cannot be accurately reflected for the real-time speed value at a point within the wave. In addition, when the motor is running at low speed, the output voltage of the tachogenerator is greatly affected by the parameters of the transistor and filter circuit in the rectifier circuit; and there will be a blind zone in the speed feedback, and the motor in the closed-loop speed regulation system will appear to jitter or even lose control, which will cause the entire control system to become unstable in severe cases. Therefore, when designing a motor control system using a tachogenerator as a feedback sensor, a wide range of accurate real-time speed measurement methods of the motor is required to ensure the performance and stability of the control system.

The current digital and networked control system is gradually applied to warp knitting machines, which has improved the information and automation level of warp knitting equipment [8-11]. Intelligent control algorithms, such as fuzzy control and neural networks have also become the core algorithms of the special control system for warp knitting machines, which has improved the intelligence level of warp knitting equipment [12]. This article provides a complete solution for the design of the multi-speed electronic let-off system for warp knitting machines. First, a wide-range digital speed measurement method is proposed which solves the problem that the traditional analog circuit speed measurement method cannot measure real-time speed, and also eliminates the problem of the low-speed feedback blind zone. Second, in view of the problem that the multi-speed electronic let-off system needs to program multiple let-off quantities, we

Ren W, Wen X, Lai S. Digital Real-Time Rotating Speed Measuring and Fuzzy PID Control Algorithm Design for the Multi-Speed Electronic Let-Off System.
FIBRES & TEXTILES in Eastern Europe 2021; 29, 4(148): 48-55. **DOI:** 10.5604/01.3001.0014.8231

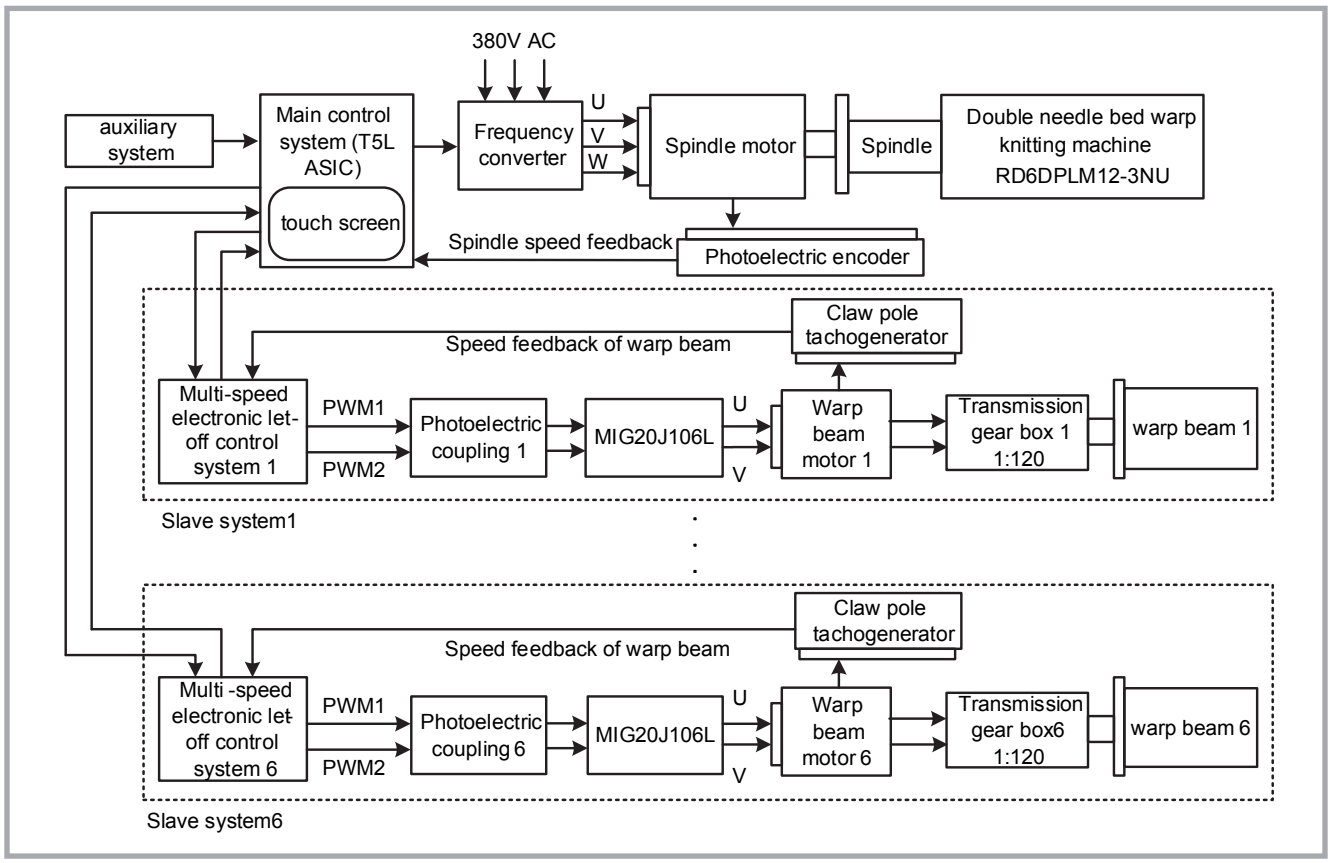

Figure 1. *Block diagram of hardware design of multi-speed electronic let-off system.*

propose a fuzzy PI speed feedback control system which can adjust the control parameters of a traditional PI controller in real time based on the fuzzy control table, so as to achieve stable speed electronic let-off.

System hardware design

The multi-speed warp knitting electronic let-off system designed in this paper adopts a modular design. The overall design framework is shown in ***Figure 1***. It is mainly composed of three parts: the main control system module, the slave electronic let-off control system module, and auxiliary system function module.

Main control system module

The main control system is based on the smart touch screen of the T5L core. T5L series ASIC (Application Specific Integrated Circuit) is a dual-core IC chip designed for AIoT (Artificial Intelligence & Internet of Things) applications, which highly integrates low-power, cost-effective GUI (Graphical User Interface) and control applications. We use T5L's CPU_GUI kernel to run the DGUS II system. The kernel has built-in high-speed video memory, with a 2.4 GBytes/S video memory bandwidth, and can achieve a high-resolution (1366 × 768) touch screen display and touch functions. Using T5L's CPU_OS kernel as the main controller, the functions realised mainly include initialising and calculating the target speed of the motor according to the process calculation results and parameters such as the outer circumference, inner circumference, let-off amount, and controller adjustment of the full beam, and sending it as a control signal to the warp beam multi-speed let-off control system. Through the equipped network module, it can realise data interaction

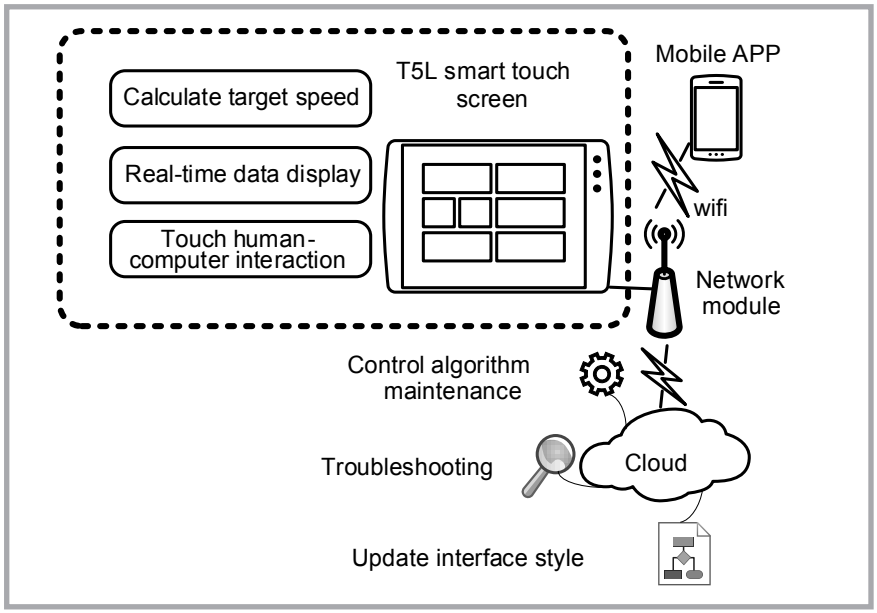

Figure 2. *Smart capacitive touch screen based on T5L core.*

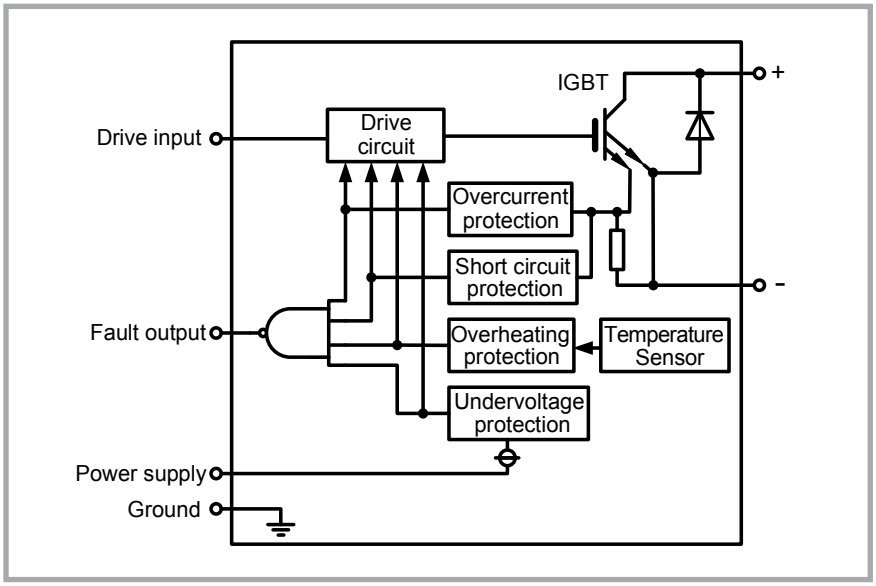

Figure 3. *Functional block diagram of MIG20J106L internal circuit.*

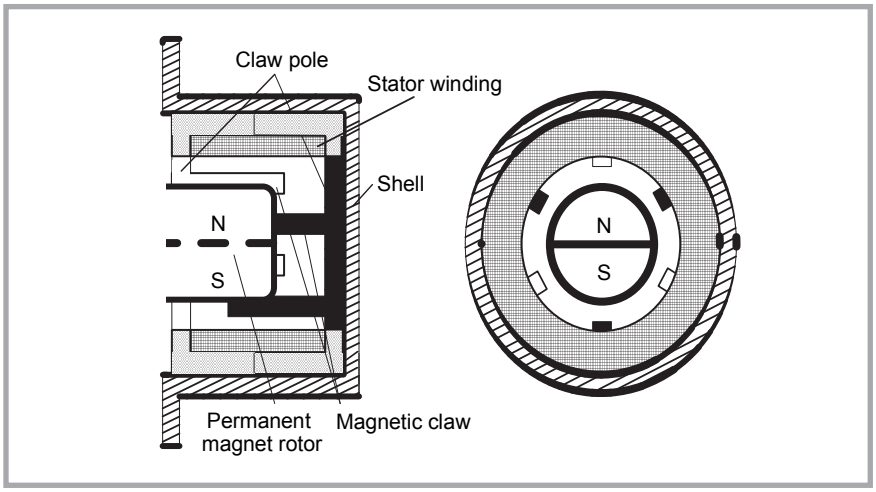

Figure 4. *Mechanical structure of claw pole permanent magnet AC tachogenerator.*

with the mobile APP, enterprise server or third-party cloud platform, realize remote maintenance of the control algorithm and online fault diagnosis, as well as update the control interface style and other functions, providing for networked production and management of multiple knitting machines. The basics are shown in ***Figure 2***.

Slave electronic let-off control system module

Six independent warp beam multi-speed electronic let-off systems are completed by the circuit design of our own design. Using a 32-bit STM32F4 microcontroller as the control core and the fuzzy PI control algorithm, according to the control signal sent by the main control system, the output PWM control signal is sent to the IPM (Intelligent Power Module) to drive the motor through the reduction gear box to drive the warp shaft to rotate, and then the pan head sends out the required yarn feeding amount to achieve high-precision and multi-speed warp let-off.

The IPM used in the design is MIG-20J106L, produced by Toshiba, Japan, and the internal circuit function principle is shown in ***Figure 3***. Its main feature is to integrate the output power components, drive circuits, and multiple protection circuits into the same module, and it can send monitored overvoltage, overheat and other fault signals to the control circuit; even if overload or improper use occurs, it can be guaranteed. Moreover, it is not damaged, greatly improving the design efficiency and increasing the reliability of the control system.

Auxiliary function system module

The auxiliary system module includes an anti-interference design and the installation of multiple sensors on the machine to realise intelligent protection, such as power failure and overheating, automatic fault detection, an alarm and other functions. The most important one is the power-down protection function, because of the fact that in the actual warp knitting production process, if there is an unexpected power failure, the host will continue to work for 3-5 seconds due to greater inertia, even though the electronic let-off system has stopped working. If the shaft has stopped feeding the yarn, it is easy for it to break, causing great losses. Secondly, fault detection is also particularly important. One situation is where it is detected that the main control system has sent a control signal to the multi-speed electronic let-off system, but the warp beam motor has not responded due to a fault, that is, the machine is working, but the warp beam has not let off. It is necessary to send a fault feedback signal to the host immediately to control the machine to stop working and send an alarm signal. There is also a situation where the electronic let-off control system fails to track the spindle accurately, and there will be a let-off error after a period of operation. Therefore, the upper limit of the deviation needs to be set, and a shutdown alarm is required after the limit is exceeded.

Wide-range digital measurement algorithm for warp beam speed

Mechanical structure and working principle of claw pole permanent magnet AC tachometer motor

The mechanical structure of the claw-pole permanent magnet AC tachometer motor is shown in ***Figure 4***, which mainly includes the shell, stator winding, claw pole, magnetic claw, permanent magnet rotor and other components.

The stator winding in the shell of the claw-pole permanent magnet AC tachometer motor is clamped and embedded between a pair of cylindrical claw poles; a rotatable permanent magnet rotor is placed in the centre of the cylindrical claw pole, and magnetic claws on the claw poles (white on the top, black on the bottom) are staggered and evenly distributed around the permanent magnet rotor.

The working principle of the claw pole permanent magnet AC tachometer motor is shown in ***Figure 5***. The permanent magnet rotor is magnetised axially, and the polarity of the magnetic poles is represented by N and S; there are 6 magnetic claws: upper claw pole (white) A, C, E and lower claw pole (black) B, D, F. The permanent magnet rotor N pole, magnetic claw A, magnetic claw D, and permanent magnet rotor S pole form a magnetic circuit as shown in ***Figure 5.a***. The direction of the magnetic field is perpendicular to the paper surface, and the induced electromotive force generated changes according to the sinusoidal law, as shown in ***Figure 5.b***.

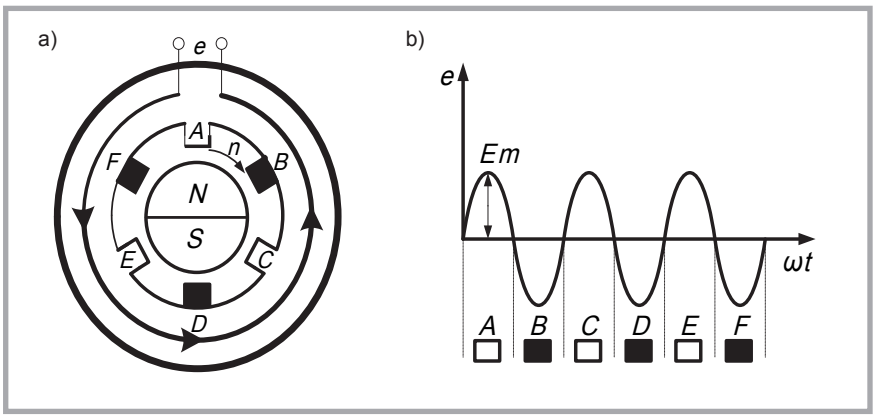

Figure 5. *Structural symmetry model of claw pole permanent magnet AC tachogenerator.*

The motor drives the permanent magnet rotor to rotate in a clockwise direction, and produces relative movement with the stator windings. According to the law of electromagnetic induction, an induced electromotive force $e(t)$ is generated in the stator winding, whose instantaneous value is:

$$e(t) = e_N(t) - e_S(t) = E(t)\sin(\omega(t)t) \quad (1)$$

Where, $E(t)$ is the maximum value of $e(t)$, $E=\pi f(t)\varphi=\omega(t)\varphi/2$, and $e_N(t)$ & $e_S(t)$ are the electromotive force of the N pole and S pole, respectively, which are equal in magnitude and opposite in direction; that is, they are different from each other by π radians in the time phase; $\omega(t)$ is the electrical angular velocity in space, $f(t)$ the frequency of $e(t)$, and φ is the air gap magnetic flux. If ω and the number of magnetic claw pairs p are known, the rotating speed n_x of the permanent magnet rotor in the clockwise direction can be expressed as:

$$n(t) = \frac{60\omega(t)}{2\pi p} \quad (2)$$

From ***Equation (2)***, we can see that the speed of the tachometer motor n_x is proportional to $\omega(t)$.

Speed estimation algorithm based on unscented kalman filter

The discrete speed model of the claw pole permanent magnet AC tachometer motor is

$$x_k = (\theta_k, \omega_k, a_k, q_k)^T \quad (3)$$

Where, θ_k is the space electrical angle parameter for the sine function in the time step k, ω_k the space electrical angular velocity in the time step k, and a_k the space electrical angular acceleration in the time step k. The values of ω_k and a_k are disturbed by one-dimensional white noise processes q_k. The measurement equation adopts the discrete form of ***Equation (1)*** with noise and can expressed as

$$e_k = \frac{\varphi}{2}\omega_k \sin(\theta_k) + r_k \quad (4)$$

Where, r_k is white, univariate Gaussian noise with a zero mean and variance $\sigma_\tau = 1$.

The specific calculation process of signal filtering using the discrete UKF (Unscented Kalman Filter) is as follows:

(1) According to the UT transformation [13], calculate the sampling point set $\chi_{k/k}$ composed of $2\tau + 1$ sigma points ***Equation (5)***.

Where, $\lambda = \alpha^2(\tau + \kappa) - \tau$ is scale factors; α and κ are both normal numbers, and α determines the distribution of sigma points around m (estimate of χ), $0 \le \alpha \le 1$. Proper adjustment of α and κ can improve the accuracy of the estimated mean value. $\left[\sqrt{(\tau+\lambda)P_{j,k|k}}\right]_i$ represents the i column of matrix $\sqrt{(\tau+\lambda)P_{j,k|k}}$, $i \in [1, 2\tau]$.

$$\begin{aligned}\chi_{k|k} = \Bigg\{ & x_{j,k|k}, x_{j,k|k} + \left[\sqrt{(\tau+\lambda)P_{jk|k}}\right]_1, \cdots, x_{j,k|k} \\ & + \left[\sqrt{(\tau+\lambda)P_{j,k|k}}\right]_\tau, x_{j,k|k} - \left[\sqrt{(\tau+\lambda)P_{j,k|k}}\right]_{\tau+1}, \\ & \cdots, x_{j,k|k} - \left[\sqrt{(\tau+\lambda)P_{j,k|k}}\right]_{2\tau} \Bigg\}\end{aligned} \quad (5)$$

$$\begin{cases} \hat{x}_{j,k+1|k} = W_m \chi_{k+1|k} \\ P_{j,k+1|k} = (\hat{x}_{j,k+1|k} - \chi_{k+1|k}) W_c (\hat{x}_{j,k+1|k} - \chi_{k+1|k})^{\mathrm{T}} + Q \end{cases}$$

$$\text{where} \begin{cases} W_m = \left[\dfrac{\lambda}{\tau+\lambda}, \overbrace{\dfrac{\lambda}{2(\tau+\lambda)}, \cdots, \dfrac{\lambda}{2(\tau+\lambda)}}^{2\tau\uparrow} \right] \\ W_c = \operatorname{diag}\left(\dfrac{\lambda}{\tau+\lambda} + (1-\alpha^2+\beta), \underbrace{\dfrac{\lambda}{2(\tau+\lambda)}, \cdots, \dfrac{\lambda}{2(\tau+\lambda)}}_{2\tau\uparrow} \right) \end{cases} . \quad (6)$$

$$\begin{aligned}\chi_{k+1|k} = \Bigg\{ & \hat{x}_{j,k+1|k}, \hat{x}_{j,k|+1k} + \left[\sqrt{(\tau+\lambda)P_{j,k+1|k}}\right]_1, \cdots, \hat{x}_{j,k+1|k} \\ & + \left[\sqrt{(\tau+\lambda)P_{j,k+1|k}}\right]_\tau, \hat{x}_{j,k+1|k} - \left[\sqrt{(\tau+\lambda)P_{j,k+1|k}}\right]_{\tau+1} \\ & \cdots, \hat{x}_{j,k+1|k} - \left[\sqrt{(\tau+\lambda)P_{j,k+1|k}}\right]_{2\tau} \Bigg\}\end{aligned} \quad (7)$$

Equations (5), (6) and (7).

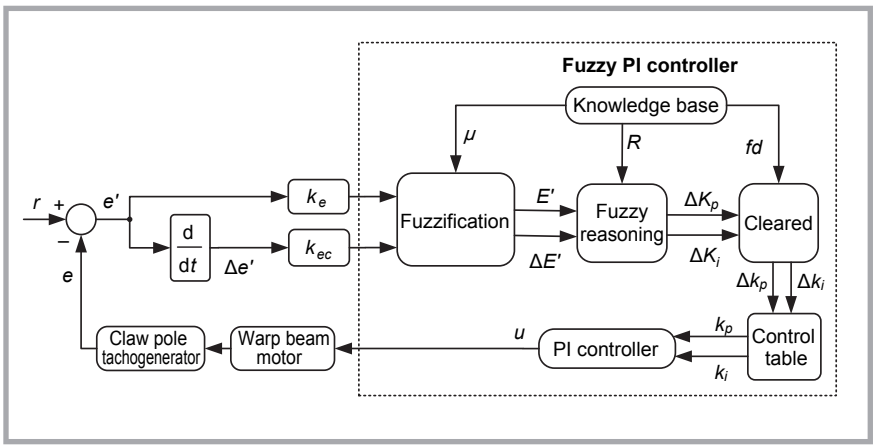

Figure 6. *Structural symmetry model of claw pole permanent magnet AC tachogenerator.*

(2) Substitute $2\tau + 1$ sigma points $[\chi_{k/k}]_i$ (i-th column of $\chi_{k/k}$, $i \in [1, 2\tau]$) into the discrete state equation of the permanent magnet rotor (3) to calculate the predicted value $\chi_{k+1/k} = f(\chi_{k/k})$ of the sampling point set $\chi_{k/k}$.

(3) The process of calculating the predicted value $\hat{x}_{j,k+1/k}$ and $P_{j,k+1/k}$ of the velocity measurement model by averaging the weighted $\chi_{k+1/k}$ is as follows ***Equation (6)***.

Where, W_m and W_c are the mean and covariance weighted values, respectively.

(4) The estimated sampling point set according to the UT transform prediction is as follows ***Equation (7)***.

(5) Substitute $2\tau + 1$ sigma point $[\chi_{k+1/k}]_i$ (the i-th column of $\chi_{k+1/k}$, $i \in [1, 2\tau]$) into the rotational speed observation ***Equation (4)*** to predict the observed value $e_{k+1/k}$, and then calculate the measurement mean $\bar{e}_{k+1/k}$, covariance $P_{e_k e_k}$, state covariance $P_{x_k e_k}$ and Kalman gain matrix K_{k+1}, the calculation method for which is as follows:

$$\begin{cases} e_{k+1|k} = h(\chi_{k+1|k}) \\ \bar{e}_{k+1|k} = W_m e_{k+1|k} \\ P_{e_k e_k} = (e_{k+1|k} - \bar{e}_{k+1|k}) W_c (e_{k+1|k} - \bar{e}_{k+1|k})^{\mathrm{T}} + R \\ P_{x_k e_k} = (\chi_{k+1|k} - \bar{e}_{k+1|k}) W_c (\chi_{k+1|k} - \bar{e}_{k+1|k})^{\mathrm{T}} \\ K_{k+1} = P_{x_k e_k} P_{e_k e_k}^{-1} \end{cases} \quad (8)$$

(6) The state and covariance of the updated model are as follows:

$$\begin{cases} \hat{x}_{j,k+1|k+1} = \hat{x}_{j,k+1|k} + K_{k+1}[e_{k+1} - e_{k+1|k}] \\ P_{j,k+1|k+1} = P_{j,k+1|k} - K_{k+1} P_{e_k e_k} K_{k+1}^{\mathrm{T}} \end{cases} \quad (9)$$

Design of fuzzy PI controller

Control principle of multi-speed let-off

According to the requirements of the warp knitting production process, the multi-speed electronic let-off system can program a variety of different sequences, and it is required that when changing from one let-off sequence to another, no obvious horizontal stripes shall be left on the cloth surface; that is, the process must be completed in one row. Therefore, when designing a multi-speed electronic let-off control program, the multi-speed let-off process is generally decomposed into two processes: sequence switching and constant-speed let-off within each sequence.

Constant speed let-off process

Assuming that the reduction of the outer circumference of the warp beam is a constant for each unwinding of the warp beam, the calculation relationship between the warp beam motor speed, let-off amount and spindle motor speed is derived as follows:

(1) Real-time circumference of warp beam:

$$L_i = L_1 - (L_1 - L_2) Z_i / Z \quad (10)$$

Where, L_i is the real-time circumference of the warp beam, L_1 the full winding circumference of the warp beam, L_2 the empty circumference of the warp beam, Z the number of windings when the warp beam is full, and Z_i is the total number of windings of the warp beam from full winding to the current moment.

(2) Target speed of warp beam motor:

$$N_1 = F N_2 T / 480 L_i \quad (11)$$

Where, N_1 is the speed of the warp beam motor, F the let-off amount, N_2 the spindle speed, and T is the speed ratio between the warp beam and the motor.

Sequence switching control

For the multi-speed let-off system, in a cycle there are multiple sequences, each of which has multiple courses (constant speed process) and corresponds to the corresponding let-off amount. When the product type is determined, the number of sequences q in a pattern cycle (each sequence contains h_i rows) and the total number of rows H are also determined accordingly

$$H = h_1 + h_2 + \ldots h_q \quad (12)$$

Therefore, after starting up, the main control system determines the current number of woven courses by recording the number of sinusoidal signal cycles of the warp beam speed, and then determines the sequence it is in. When it is judged that all the courses required by the current sequence have been knitted, the constant speed let-off process is ended. According to the technological requirements, the speed of the warp beam motor is quickly adjusted in the next course, so as to enter the next sequence smoothly.

Fuzzy PI control algorithm of multi-speed electronic let-off system

The core of the multi-speed let-off control algorithm is a dual-input and three-output fuzzy PI controller based on the Mamdani model. The structure is shown in ***Figure 6***.

Suppose the desired value of the warp beam speed is r, the measured value of the warp beam speed is e, the temperature error $e' = r - e$, and the temperature error change rate $\Delta e'$ is the reciprocal of e'. The proportional and integral adjustment parameters are $k_p = k_{p0} + \Delta k_p$ and $k_i = k_{i0} + \Delta k_i$, respectively, where k_{p0} and k_{i0} are initial values, and Δk_p and Δk_i are adjustment variables. The input of the fuzzy PI controller is the quantised clear value of e' and $\Delta e'$, and the output is the control variable U. E' and $\Delta E'$ are the fuzzy variables corresponding to e' and $\Delta e'$, respectively, and ΔK_p and ΔK_i are those corresponding to Δk_p and Δk_i, respectively. The quantisation factors of the scale transformation are k_e and k_{ec}, respectively. In order to reduce the dimensionality of the control algorithm,

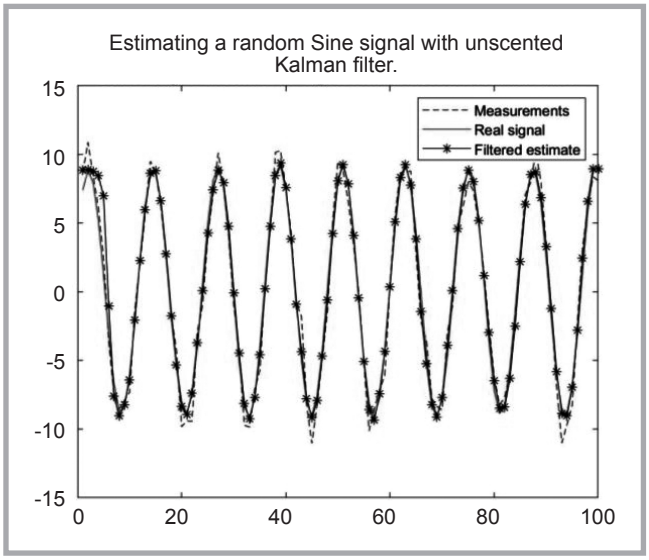

Figure 7. *Test result of constant speed let-off.*

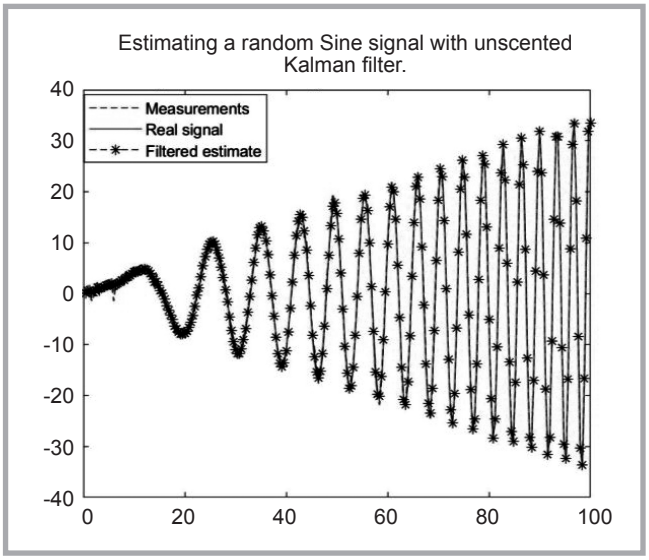

Figure 8. *Uniformly accelerated let-off test results.*

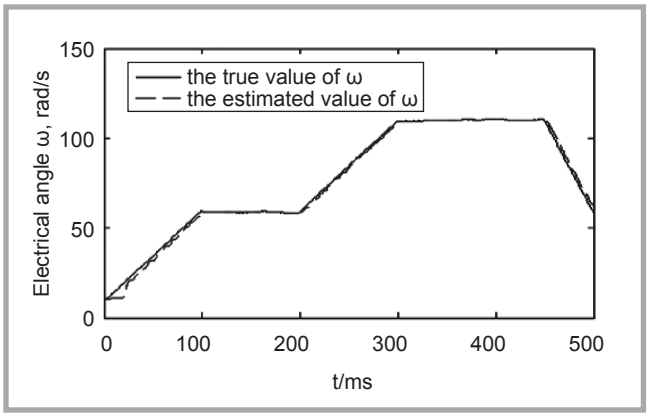

Figure 9. *Estimated curve of electrical angular velocity ω.*

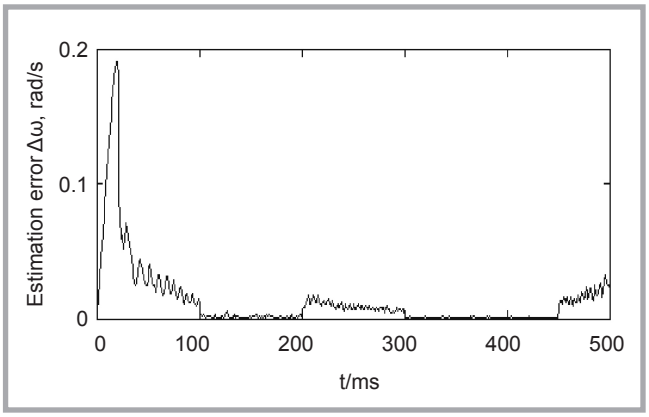

Figure 10. *Error estimation curve of electrical angular velocity ω.*

when we construct the fuzzy inference relationship, we select the absolute value of the input and output variables of the fuzzy PI controller. The main construction principles and techniques are as follows:

(1) When $|e'|$ is large, in order to speed up the response speed of the system, a larger k_p should be used to reduce the time constant and damping coefficient of the system. In order to avoid large overshoot, the integral effect can be removed and $k_i = 0$ is taken.

(2) When $|e'|$ is in a medium size, a smaller k_p should be used to reduce the overshoot of the system; at this time, k_i can be increased a little, but not by too much.

(3) When $|e'|$ is smaller, in order to make the system have good steady-state performance, k_p and k_i can be larger.

According to the qualitative relationship between the above $|e'|$ and parameters k_p and k_i, combined with the influence of $|\Delta e'|$, the fuzzy control rules of the PI controller are as shown in ***Table 1*** and ***Table 2***.

Simulation analysis

MATLAB software was used to verify the simulation. ***Figure 7*** shows the effectiveness of the wide-range digital speed measurement algorithm based on

Table 1. *Fuzzy control rules for adjusting k_p.*

Δk_p		|e|			
		L	**M**	**S**	**ZO**
|ec|	L	M	S	M	M
	M	L	M	L	L
	S	L	M	L	L
	ZO	L	M	L	ZO

Table 2. *Fuzzy control rules for adjusting k_i.*

Δk_i		|e|			
		L	**M**	**S**	**ZO**
|ec|	L	ZO	S	M	L
	M	ZO	S	L	L
	S	ZO	ZO	L	L
	ZO	ZO	ZO	L	ZO

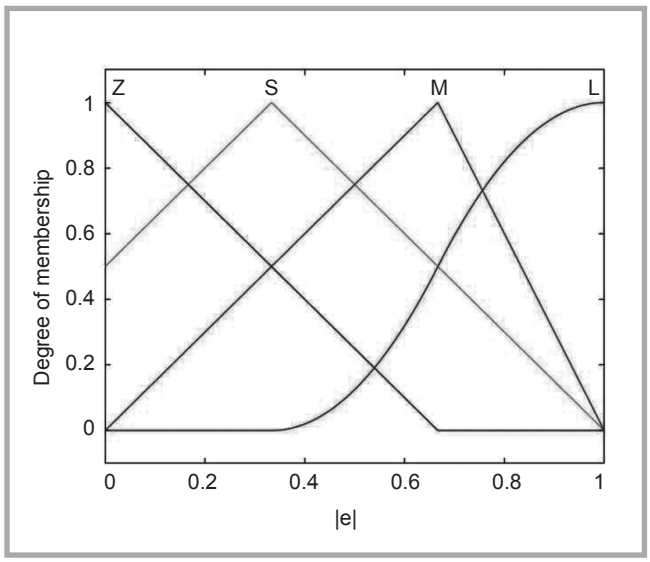

Figure 11. *Membership function.*

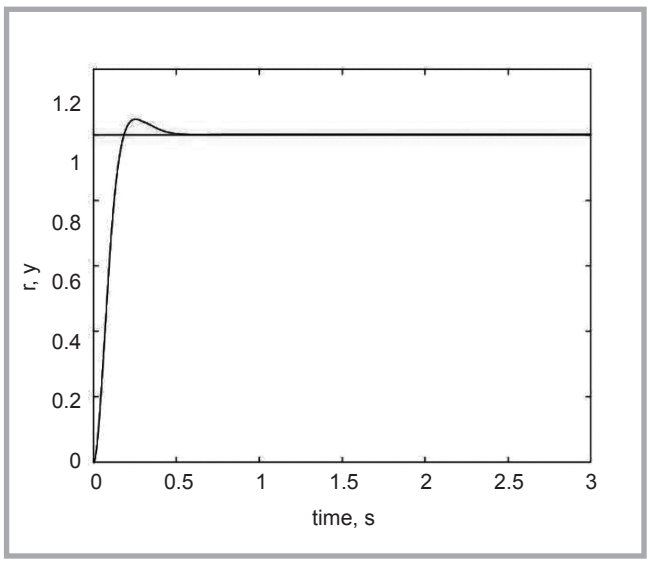

Figure 12. *Speed tracking curve using fuzzy PI control algorithm.*

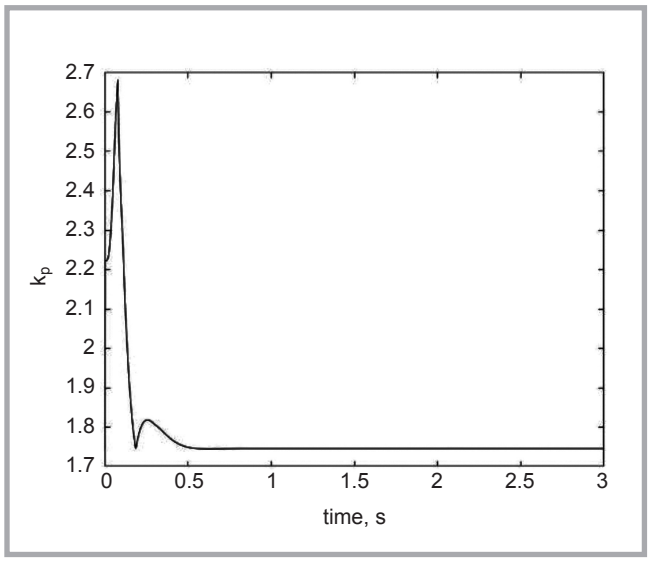

Figure 13. *Fuzzy adaptive adjustment process of k_p.*

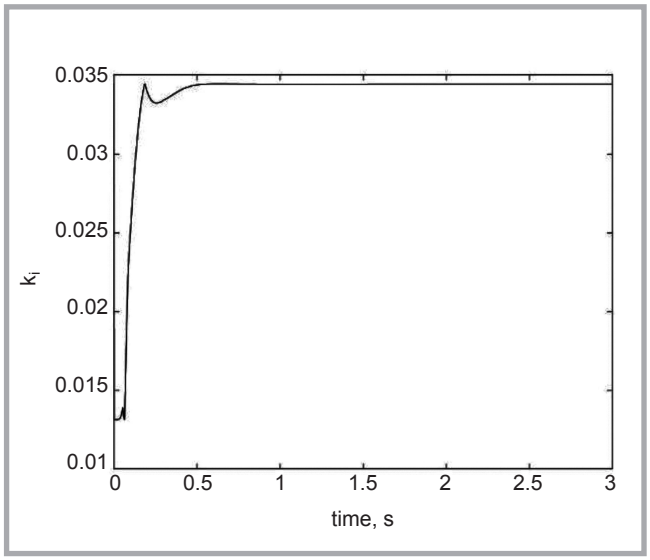

Figure 14. *Fuzzy adaptive adjustment process of k_i.*

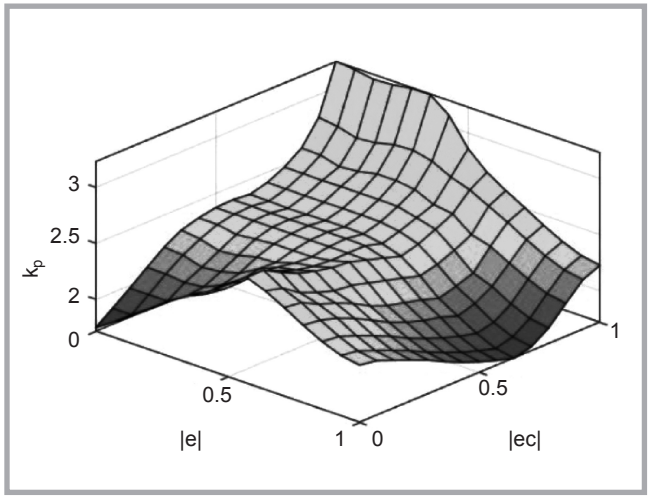

Figure 15. *Surface of k_p.*

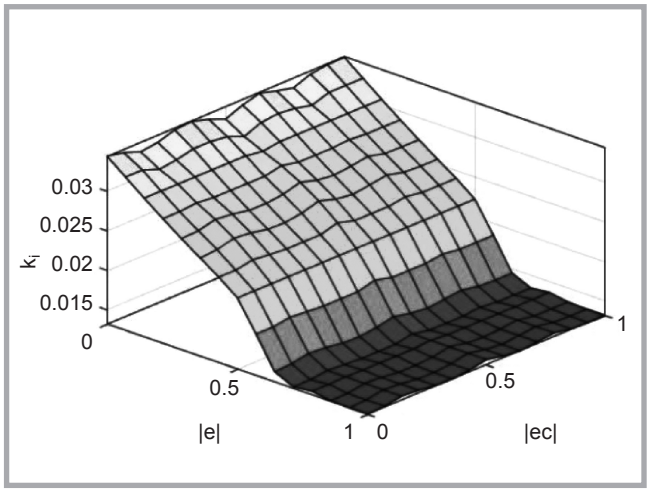

Figure 16. *Surface of k_i.*

the UKF filter algorithm proposed in this paper. The simulation results in ***Figure 8*** show that the speed measurement algorithm is suitable for multi-speed electronic let-off systems. ***Figure 9*** shows that the electrical angle ω can be estimated using a sine form of the measurement model. ***Figure 10*** shows the error estimation curve of the electrical angular velocity ω.

When the fuzzy PI control algorithm is used to realise the multi-speed electronic let-off algorithm, k_p, k_i, $|e'|$ & $|\Delta e'|$ all adopt the membership function, as shown in ***Figure 11***. ***Figure 12*** shows the speed tracking curve using the fuzzy PI control algorithm, which verifies the effectiveness of the fuzzy PI algorithm. ***Figures 13-16*** show the fuzzy adaptive adjustment process of k_p and k_i, which is suitable for multi-speed electronic let-off system. Through the graphs shown in ***Figures 15*** and ***16***, it can be seen that the fuzzy PI control algorithm designed has excellent performance. ***Figure 17*** shows the generation process of the fuzzy control table. For example, when $|e'| = 0.5$ and $|\Delta e'| = 0.5$, $k_p = 2.37$ and $k_i = 0.02$ can be inferred by fuzzy inference, consequently a fuzzy control table of k_p and k_i can be established. Input the fuzzy control table into the microcontroller to realise a high-efficiency and low-calculation fuzzy PI control algorithm for the embedded system.

Conclusions

This article presents a complete design method for a fully digital multi-speed electronic let-off system for warp knitting machines. The design content covers the hardware system and software algorithm design. We formulated an integrated design for the speed measurement system and intelligent control system. The real-time speed measurement system based on UKF solves the problem that the traditional analog circuit speed measurement method cannot measure the real-time speed. The fuzzy PI intelligent control algorithm designed provides a useful engineering design reference for realising a multi-speed electronic let-off system for warp knitting machines.

Conflict of interests

The authors declare that there is no conflict of interest regarding the publication of this paper.

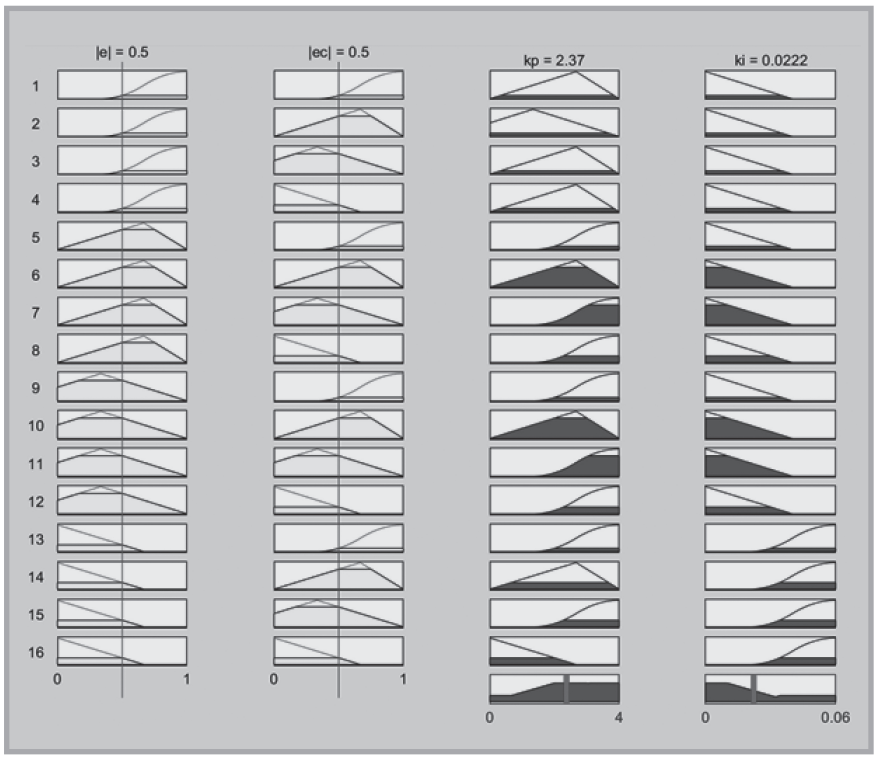

Figure 17. *Fuzzy rule trigger distribution.*

Acknowledgments

This work was supported by the Key Industrial Guidance Projects of Fujian Province (2019H0034).

References

1. Wang W, Jiang G. Control Process and Algorithm on Warp Knitting Multi-Speed Electronic Let-Off System. *Journal of Textile Research* 2007; 28(9): 110-113.
2. Mayer K. EBA 2-Step Documentation (Version 3.0). Karl Mayer Textilmaschinen fabric GmbH, 2000(5): 31-32.
3. Zhang Q, Jiang G, Xia F, et al. Choice and Dynamic Response Analysis of Control Model for Electronic Shogging Motion on Highspeed Warp Knitting Machine. *Journal of Textile Research* 2012; 33(1): 126-131.
4. Offermann P. Warp Knitting Machines. *International Textile Bulletin* 2003; 49, 6: 52-53.
5. Yang SH, Lorenz RD. Surface Permanent-Magnet Machine Self-Sensing at Zero and Low Speeds Using Improved Observer for Position, Velocity And Disturbance Torque Estimation. *IEEE Transactions on Industry Applications* 2012; 48(1): 151-160.
6. Yang YP, Ting YY. Improved Angular Displacement Estimation Based on Hall -Effect Sensors for Driving a Brushless Permanent Magnet Motor. *IEEE Transactions on Industrial Electronics* 2014; 61(1): 504-511.
7. Hagiwara N, Suzuki Y, Murase H. A Method of Improving the Resolution and Accuracy of Rotary Encoders Using a Code Compensation Technique. *IEEE Transactions on Instrumentation and Measurement* 1992; 41(1): 98-101.
8. Zhang Q, Jiang G, Xia L. Development of Key Technologies for Warp-Knitting Machine CNC System. *China Textile Leader* 2013; 4: 77-80.
9. Yang R, Bewick S, Zhang M, et al. Adaptive Immune System TH1/TH2 Differentiation Mechanism Inspired Perimeter Patrol Control Strategy. *IEEE Transactions on Control Systems Technology* 2011; 19(2): 407-415.
10. Lai S, Ren W. The Design of Electronic Jacquard Hybrid Isomerism Serial Communication System for Warp Knitting Machine. *Chinese Journal of Engineering Design* 2017; 24(3): 343-349, 358.
11. Ravenhorst JHV, Akkerman R. A Yarn Interaction Model for Circular Braiding. Composites Part A: Applied Science and Manufacturing 2016; 81: 254-63.
12. Ren W, Xu B. Development of Multi -Speed Electric Let-Off System for Warp Knitting Machine Based on FI-SNAPID Algorithm. *Journal of Zhejiang University* 2013; 47(10): 1715-1718.
13. Zhao Z, Zhu Q, Zhou L, et al. Vehicle Speed Estimation in Driving Case Based on Distributed Self-Adaptive Unscented Kalman Filter for 4WD Hybrid Electric Car. *Scientia Sinica Technologica* 2016; 46(5): 481-492.

Received 18.02.2020 Reviewed 15.02.2021